Personalised Models of Atrial Propagation Fitted to Clinically-Induced Activation Maps

Duna de Luis-Moura[1], Chiara Celotto[2], Saman Golmaryamii[3], María Termenón-Rivas[1], Giada S Romitti[1], Etel Silva[3], Juan Fernandez-Armenta[3], José F Rodriguez[2], Alejandro Liberos[1], Miguel Rodrigo[1]

[1]CoMMLab, Universitat de València,València, Spain
[2]Department of Chemistry Giulio Natta, Politecnico di Milano, Milano
[3]Department of Cardiology, Hospital Universitario Puerta del Mar, Cádiz, Spain

Abstract

Atrial fibrillation (AF) is the most common cardiac arrhythmia, and its treatment by ablation still presents variable results among patients. In this paper, we present a personalised simulation methodology fitted to clinical data to improve understanding of the atrial electrical substrate and support clinical decision making.

We analysed high-density electro-anatomical mapping signals recorded during a triple extra-stimulus protocol able to reveal conduction disturbances on atrial tissue. Computed tomography data was used to build patient-specific 3D atrial models in which electrophysiological simulations were performed and adjusted to reproduce clinical local activation maps (LAT) maps. These included an adjustment of tissue propagation properties and electrical remodelling, to reproduce different levels of disease progression.

This methodology reproduced both inter-individual and regional variation in atrial propagation conditions during the triple extra-stimuli. Simulated LAT maps reproduced clinical data with 23.4 ms average deviation, and were better reproduced in patients with lower heterogeneity between LAT maps.

1. Introduction

Atrial fibrillation (AF) is the most common cardiac arrhythmia and is associated with rapid and irregular activation of the atria [1]. Although pulmonary vein isolation (PVI) is an effective therapy, many patients with persistent AF experience recurrences [2, 3]. This has prompted the need to identify more precisely the regions responsible for arrhythmia maintenance in order to optimise ablation strategies.

With the aim of revealing non-obvious conduction disturbances on the atrial tissue, electrophysiological biomarkers can be extracted from specific pacing protocols, such using three extra-stimuli (3-Extra) with pacing intervals close to the effective refractory period. These stimuli are administered at short, decreasing intervals, inducing electrical responses that reveal regions of abnormal conduction, such as double or highly fragmented electrograms. These pathological regions could therefore be considered potential targets for catheter ablation strategies [4].

In this context, personalised computational models are a promising tool in precision cardiology. By reproducing the specific anatomy and electrophysiology of each patient, these models allow different pacing scenarios to be explored and their effect on the propagation of atrial activation to be observed [5]. The aim of the present study was to generate personalized simulations of AF patients to simulate the 3-Extra protocol and evaluate their ability to reproduce clinical local activation time (LAT) maps, as a preliminary step to the development of individualised therapeutic strategies.

2. Materials and Methods

2.1. Clinical Data

Data from four patients with persistent atrial fibrillation (P001, P005, P006 and P008), included in a prospective study conducted at the Hospital Universitario Puerta del Mar (Cádiz, Spain), were analysed. Computed tomography (CT) scan was used to generate left atrial (LA) wall thickness maps and to segment their individual anatomical structures. In addition, high-density electro-anatomical mapping was performed using the CARTO3 system and a PentaRay® catheter. Intracardiac signals (EGMs) were recorded in two conditions: during sinus rhythm (SR) and during the application of a triple extra-stimulus protocol (Fig. 1), consisting of three sequential electrical with values close to atrial effective refractory period (AERP): at AERP + 60 ms, AERP + 40 ms and AERP + 30 ms.

Stimuli were applied from the distal coronary sinus (CS) or from the left atrial appendage (LAA), with the aim of revealing regions with electrical conduction disturbances that may be relevant to the ablation strategy. Signals recorded during the 3-Extra protocol, with a duration of 2.5 seconds each, were used to calculate local activation maps (LAT) corresponding to each of the three pulses as the maximal absolute amplitude in bipolar EGMs. These maps served as a reference to validate and adjust the results of the computational simulations. Clinical LAT map variability was also estimated for each patient by computing the mean absolute difference in LAT values across all pairs of clinical LAT maps.

2.2. Simulation Models

From the three-dimensional meshes of each patient's LA, volumetric models composed of tetrahedral elements (0.4 mm resolution) were generated, which served as the basis for the electrical simulations (Fig. 1). Simulations were performed using a GPU-based biophysical solver with a fixed time step of 0.02 ms [6]. The Koivumäki atrial cellular model was used, including the effect of electrical remodelling [7]. To reproduce different degrees of disease progression associated with AF, electrical remodelling was included as a parameter, where 0% remodelling represented healthy tissue and 100% or upper remodelling factors corresponded to a chronic AF cellular model: SERCA expression (-16%), PLB to SERCA ratio (+18%), SLN to SERCA ratio (-40%), maximal I_{NCX} (+50%), sensitivity of RyR to [Ca2+], SR (+100%), conductance of I_{CaL} (-59%), conductance of I_{to} (-44%), conductance of I_{Kur} (-22%) and conductance of I_{K1} (+100%). Basal conduction anisotropy features were included [8, 9], changes on properties of electrical propagation were simulated both global and locally by increasing or decreasing the local diffusion tensor of the mesh.

Sinus rhythm stimuli was applied in the upper region of the Bachmann Bundle (BB) of the LA, while the 3-Extra stimuli were applied in the same location as in the patients (LAA or CS). Each simulation lasted for 2,5 seconds, including three SR stimuli (600 ms period) and the posterior 3-Extra stimuli, under the same duration conditions as in patients. With the simulated transmembrane potential signals, LAT maps were generated identifying maximal dV/dt instants.

2.3. Simulation Adjustment

Simulation fitting to clinical LAT data was performed in several stages. First, different degrees of global diffusion, understood as homogeneous modifications in the propagation properties of the atrial tissue, were explored to reproduce the propagation patterns observed on the first extra-stimuli LAT map. Then, a local adjustment was performed, by including spatially heterogeneous modification of the tissue diffusion, depending on the difference between the simulated and clinically recorded LAT measures or each atrial region for the first extra-stimuli. Finally, once the diffusion field was adjusted on the first extra-stimuli, different global electrical remodelling factors were evaluated to select the configuration, as the one providing minimal mean absolute error (MAE) between clinical and simulated LAT maps on the three extra-stimuli.

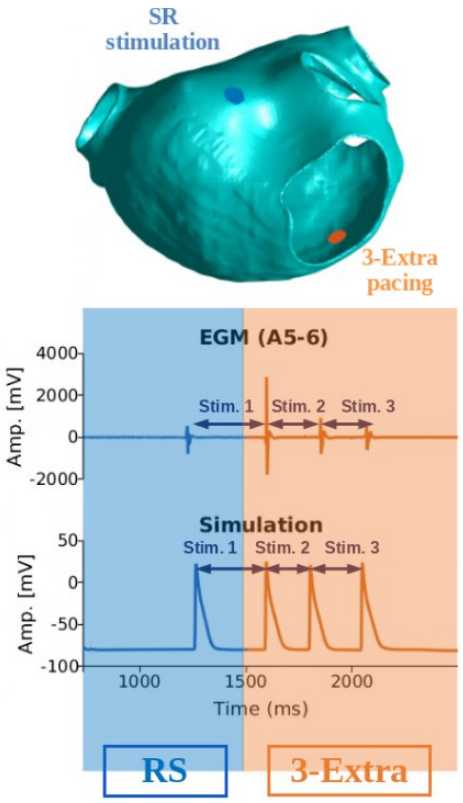

Figure 1. Location of stimulation points in the LA (up) and examples of clinical (EGM) and simulated AP signals (bottom).

3. Results

As an illustrative example of the adjustment and validation process, the results obtained for two patients with different levels of variability in their activation maps are presented in Figures 2 and 3. The upper part of the figure shows the LAT maps obtained from the clinical data (left) and from the simulations (right), in posterior view, for each of the three stimuli.

Figure 2 shows the results for patient P008 whose clinical LAT maps show a high stability between the three stimuli applied during the 3-Extra protocol (variability of 5.1 ± 3.3 ms). This consistency facilitated their reproduction by simulations, resulting in a good fit

between simulations and the real data (average MAE of 17.7 ms). The MAE curves for each LAT are shown as a function of the percentage of remodelling applied (Fig 2.B), where the optimal MAE was obtained with 125% remodelling, corresponding to progressed AF. In this case, large values of electrical remodelling (>50%) allowed to better reproduce the LAT maps, and low remodelling values (healthier tissue) worsened the reproduction of clinical maps.

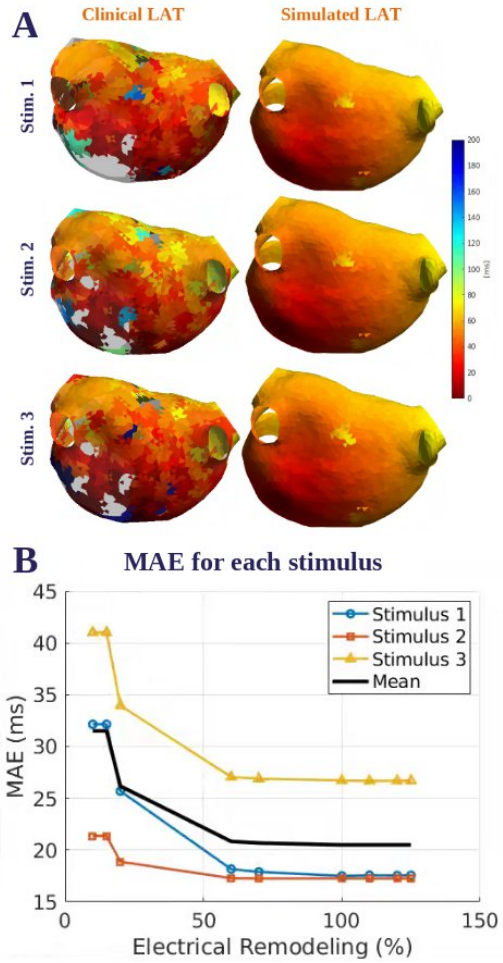

Figure 2. A) Clinical (left) and simulated (B) LAT maps for patient P008. B) Error on LAT simulation as a function of global electrical remodelling.

Figure 3 illustrates the results for patient P006 which had a higher variability between the LAT maps derived from clinical data (variability of 18.9 ± 9.7 ms). This case represents a more challenging scenario, where the simulation managed to partially capture the complexity observed in the clinical data. Fig. 3A shows the six corresponding maps (triple stimuli LAT map from the clinical data on left and from simulation on right), from a posterior view. Curves of MAE as a function of the applied remodelling showed the optimal remodelling value was obtained of 15%, for an average MAE of 20.5 ms, although with different trends for the three extra-stimuli. Reducing the electrical remodelling allowed to better reproduce the second and third stimuli LAT, however with different responses for low remodelling values.

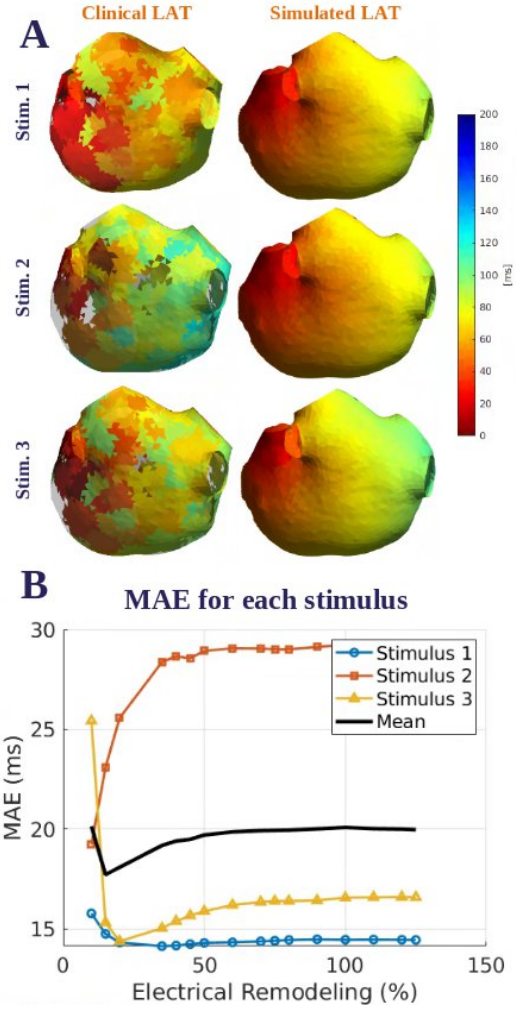

Figure 3. A) Clinical (left) and simulated (B) LAT maps for patient P006. B) Error on LAT simulation as a function of global electrical remodelling.

Errors between simulated and clinical LAT maps for each patient and for each of the three LAT maps are shown in Figure 4. Average MAE errors were smaller for the first extra-stimuli (14.5 ± 2.5 ms) compared with the second and third extra-stimuli (28.5 ± 13.6 ms and 22.0 ± 6.7 ms respectively), consequence of adjusting the diffusion on the first stimuli. Patients P005, P006 and P008 allowed better LAT simulation (18.6 ms, 17.7 ms and 20.5 ms respectively), compared with patients P001 (30.5 ms), which was correlated with the LAT variability intra-patient (P005: 16.6 ± 9.4 ms; P006: 18.9 ± 9.7 ms; P008: 5.1 ± 3.3 ms; P001: 28.6 ± 12.0 ms). The average MAE across all patients and maps was 23.4 ms.

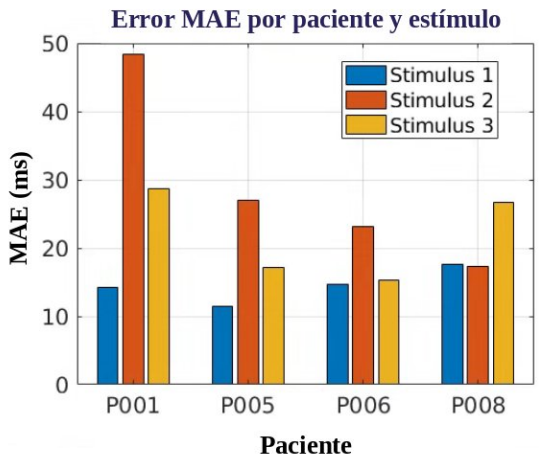

Figure 4. Error in LA simulation for all patients and stimulus.

4. Discussion and Conclusions

The proposed workflow allowed to extract anatomical and electrophysiological biomarkers related with the atrial substrate, in form of LAT maps of three close-to-refractory period stimulate. These biomarkers were then used to adjust patient-specific biophysical simulations able to reproduce the variability of clinical LAT map. Patients with stable LAT maps allowed a reliable fit between simulation and clinical biomarkers, although patients showing heterogeneity in their LAT maps resulted in larger simulation deviation respect to clinical LATs.

To perform the biophysical model fitting to the clinical LAT maps, electrical diffusion and remodelling were used. The first allowed to adapt the propagation conditions of the atrial substrate, and electrical remodelling allowed to introduce variability between the three extra-stimuli maps as changes in the effective refractory period and conduction velocity due to cellular remodelling. This differentiation allowed fitting both the global pattern and the functional differences to different stimuli, improving model customisation.

This workflow will be improved by the inclusion of other important substrate characteristics, such as fibrosis infiltration. This parameter will allow to better reproduce local changes in conduction properties. Furthermore, this workflow will be extended beyond the limited number of patients included in this manuscript.

Overall, this methodology is a step towards personalised simulation as a clinical support tool. Patient-specific simulations reproducing electrophysiological biomarkers will allow to better characterize the atrial substrate favouring AF initiation and maintenance, aiming to study potential fibrillatory mechanisms and targets for therapy through realistic simulations.

Acknowledgments

This work was funded by Generalitat Valenciana Grant AICO/2021/318 (Consolidables 2021), Grants PID2020-114291RB-I00, PID2023-148702OB-I00 and EraNet PCI2024-153442 funded by MCIN/ 10.13039/501100011033 and by “ERDF A way of making Europe”.

References

[1] Brundel BJJM, Ai X, Hills MT, Kuipers MF, Lip GYH, de Groot NMS, (2022). Atrial fibrilation. Nat Rev Dis Primers, 8(1):21

[2] Haissaguerre, M., Jaïs, P., Shah, D. C., Takahashi, A., Hocini, M., Quiniou, G., ... & Clémenty, J. (1998). Spontaneous initiation of atrial fibrillation by ectopic beats originating in the pulmonary veins. New England Journal of Medicine, 339(10), 659-666.

[3] Prystowsky, E. N., Padanilam, B. J., & Fogel, R. I. (2015). Treatment of atrial fibrillation. Journal of the American Medical Association (JAMA), 314(3), 278-288.

[4] Silva Garcia, E., Lobo-Torres, I., Fernandez-Armenta, J., Penela, D., Fernandez-Garcia, M., Gomez-Lopez, A., ... & Berruezo, A. (2023). Functional mapping to reveal slow conduction and substrate progression in atrial fibrillation. Europace, 25(11), euad246.

[5] Cluitmans, M. J., Plank, G., & Heijman, J. (2024). Digital twins for cardiac electrophysiology: state of the art and future challenges. Herzschrittmachertherapie + Elektrophysiologie, 35(2), 118-123.

[6] García-Mollá, V. M., Liberos, A., Vidal, A., Guillem, M. S., Millet, J., Gonzalez, A., ... & Climent, A. M. (2014). Adaptive step ODE algorithms for the 3D simulation of electric heart activity with graphics processing units. Computers in Biology and Medicine, 44, 15-26.

[7] Koivumäki, J. T., Seemann, G., Maleckar, M. M., & Tavi, P. (2014). In silico screening of the key cellular remodeling targets in chronic atrial fibrillation. PLOS Computational Biology, 10(5), e1003620.

[8] A. Liberos, M. Rodrigo, I. Hernandez-Romero, A. Quesada, F. Fernandez-Aviles, F. Atienza, A. M. Climent y M. S. Guillem, (2019). Phase singularity point tracking for the identification of typical and atypical flutter patients: A clinical-computational study. Computers in biology and medicine, 104, 319-328.

[9] M. W. Krueger, V. Schmidt, C. Tobón, F. M. Weber, C. Lorenz, D. U. Keller, H. Barschdorf, M. Burdumy, P. Neher, G. Plank, K. Rhode, G. Seemann, D. Sanchez-Quintana, J. Saiz, R. R. y O. Dössel, (2011, May). Modeling Atrial Fiber Orientation in Patient-Specific Geometries: A Semi-automatic Rule-Based Approach. In International conference on functional imaging and modeling of the heart (pp. 223-232). Berlin, Heidelberg: Springer Berlin Heidelberg.

Address for correspondence:

Miguel Rodrigo
Av. de la Universitat s/n 46100 Burjassot. Valencia. Spain.
miguel.rodrigo@uv.es